

Natural Product Research

Formerly Natural Product Letters


ISSN: (Print) (Online) Journal homepage: <https://www.tandfonline.com/loi/gnpl20>


Imperatorin from the aerial parts of *Cleome viscosa* L.: a characterization study and evaluation of the antibacterial activity

Govindan Lakshmanan, **Ammar B. Altemimi**, C. Sivaraj, Jeyaperumal Selvakumari, L. Karthik, K. Saravanan, Vijay Viswanathan, Arjun Pandian, Francesco Cacciola, Marwa Rashad Ali, Mazin A. A. Najm & Tarek Gamal Abdelmaksoud

To cite this article: Govindan Lakshmanan, Ammar B. Altemimi, C. Sivaraj, Jeyaperumal Selvakumari, L. Karthik, K. Saravanan, Vijay Viswanathan, Arjun Pandian, Francesco Cacciola, Marwa Rashad Ali, Mazin A. A. Najm & Tarek Gamal Abdelmaksoud (2023): Imperatorin from the aerial parts of *Cleome viscosa* L.: a characterization study and evaluation of the antibacterial activity, Natural Product Research, DOI: [10.1080/14786419.2023.2190116](https://doi.org/10.1080/14786419.2023.2190116)

To link to this article: <https://doi.org/10.1080/14786419.2023.2190116>

 View supplementary material 

 Published online: 28 Mar 2023.

 Submit your article to this journal 

 View related articles 

 View Crossmark data 

SHORT COMMUNICATION



Imperatorin from the aerial parts of *Cleome viscosa* L.: a characterization study and evaluation of the antibacterial activity

Govindan Lakshmanan^{a,b}, Ammar B. Altemimi^{c,d}, C. Sivaraj^e,
Jeyaperumal Selvakumar^f, L. Karthik^g, K. Saravanan^h, Vijay Viswanathanⁱ,
Arjun Pandian^j, Francesco Cacciola^k, Marwa Rashad Ali^l, Mazin A. A.
Najm^m and Tarek Gamal Abdelmaksoud^l

^aCentre for Advanced Studies in Botany, University of Madras, Chennai, India; ^bDepartment of Anatomy, Saveetha Medical College and Hospital, Institute of Medical and Technical Sciences, Chennai, Tamil Nadu, India; ^cDepartment of Food Science, College of Agriculture, University of Basrah, Basrah, Iraq; ^dCollege of Medicine, University of Warith Al-Anbiyaa, Karbala, Iraq; ^ePhytochemistry and Natural Product, ARMATS Biotek Training and Research Institute, Chennai, India; ^fDirectorate of Health & Family Welfare Services, Integrated Disease Surveillance Program, Puducherry, India; ^gCentral Research Laboratory, ToxiVen Biotech Private Limited, Kovaiipudur, Tamil Nadu, India; ^hDepartment of Physics, Periyar University, Salem, Tamil Nadu, India; ⁱDepartment of Biophysics, All India Institute of Medical Sciences (AIIMS), New Delhi, India; ^jDepartment Research and Innovation, Institute of Biotechnology, Saveetha School of Engineering (SSE), Saveetha Institute of Medical and Technical Sciences (SIMATS), Chennai, Tamil Nadu, India; ^kDepartment of Biomedical, Dental, Morphological and Functional Imaging Sciences, University of Messina, Messina, Italy; ^lFood Science Department, Faculty of Agriculture, Cairo University, Giza, Egypt; ^mPharmaceutical Chemistry Department, College of Pharmacy, Al-Ayen University, Thi-Qar, Iraq

ABSTRACT

Cleome viscosa L., a member of the family Cleomaceae, is a potential medicinal plant, known for several bioactive properties such as: anticancer, antidiabetic, antioxidant, anti-inflammatory, antimicrobial, wound healing, etc. Our study aimed to isolate a bioactive compound and assess its antibacterial activity. The crystal compound imperatorin was isolated and reported for the first time from the aerial parts of *C. viscosa*. The isolation was made using silica gel (100–200 mesh) column chromatography. The structure of imperatorin was investigated through single-crystal XRD, unit cell molecules, FTIR, and ESI-MS spectral analysis. The results validated imperatorin's triclinic crystal structure and P2₁/c distance group. The electronic structure was also calculated (4.28/6.21 D) along with the frontier molecular orbital, dipole moment, atomic charges, and electrostatic map of particles in gaseous stage and active site. Imperatorin showed highest activity at 40 µg/mL concentration against Gram +ve bacteria: *Staphylococcus aureus* (3 ± 0.2 mm), *Bacillus subtilis* (3 ± 0.6 mm), and Gram -ve bacteria: *Klebsiella pneumoniae* (3 ± 0.2 mm), *Escherichia coli* (5 ± 0.2 mm). The study highlights that the compound can be isolated in larger quantities as the plant is easily available across the tropics.

ARTICLE HISTORY

Received 17 January 2023

Accepted 7 March 2023

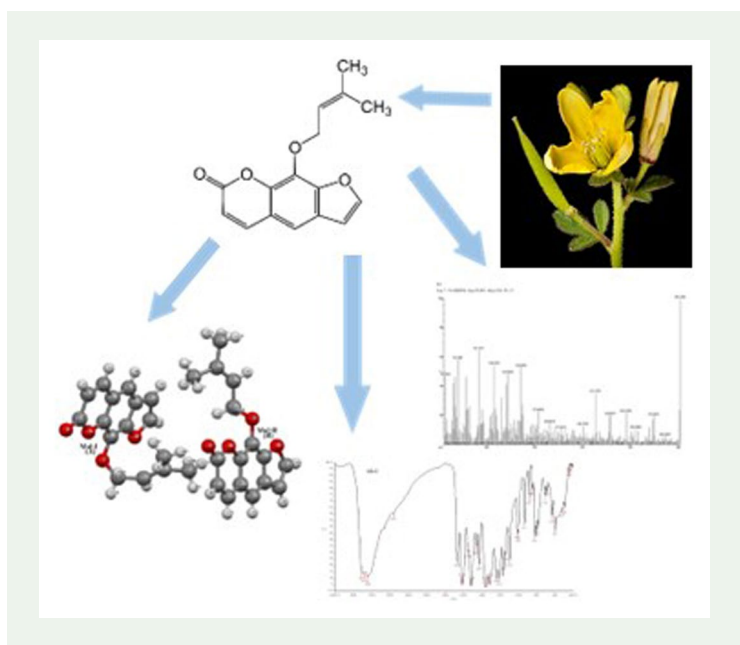
KEYWORDS

Cleome viscosa;
imperatorin;
single crystal-XRD;
antibacterial activity

CONTACT Govindan Lakshmanan ✉ lakshmanang261988@gmail.com lakshmanang.smc@saveetha.com; Francesco Cacciola ✉ cacciola@unime.it

Supplemental data for this article can be accessed online at <https://doi.org/10.1080/14786419.2023.2190116>.

© 2023 Informa UK Limited, trading as Taylor & Francis Group



1. Introduction

Diseases are generating major health difficulties worldwide. Globally, natural products are in major demand to treat diseases in developed and developing countries, and their treatment is a struggle with some successful cases (Ekor 2014). Herbs are natural products free from side effects, easily available, low-cost, and eco-friendly. Many diseases may be potentially cured with natural remedies where an important role is played by flavonoids, phenolic compounds, etc. Plants do contain several secondary metabolites such as alkaloids, steroids, phenols, fatty acids, essential oils, flavonoids, anthocyanins, and terpenes also significant in various biological studies (Singh et al. 2017). The human population has increased more than 80% worldwide, and based on the human population the requirement and consumption increased for medicine, agricultural, pharma industry and food, etc. (Ekor 2014).

Cleome viscosa L. belongs to one of the largest genera under the family Cleomaceae (formerly Capparidaceae). *C. viscosa* generally known as “duckweed or wild dog mustard”, is a pantropical yearly medicinal plant gummy herb (found in India all over the plains) (Phan et al. 2016). It is a significant conventional plant for Indian-Ayurvedic and the Chinese remedy system, used in different aspects such as blood diseases, and uterine complaints, hypertension, rheumatic arthritis, snake bite, neurasthenia, malaria, and wound healing and for its anti-inflammatory, analgesic-antipyretic, anthelmintic, hypoglycemic, hepatoprotective, and antidiarrhoeal activities (Yadav et al. 2010). It is used in traditional medicine as nutritional supplement due to the most abundant resource of bioactive constituents (Ahmed et al. 2011). Previously, several bioactive compounds have been isolated from *C. viscosa* such as viscoside A, B, flavonol glycosides, kaempferitrin, vincetoxicoside A, B, kaempferol 3-O-b-D-glucopyranoside

7-O-a-L-rhamnopyranoside, kaempferide 3-O-b-D-glucopyranoside 7-O-a-L-rhamnopyranoside, and isorhamnetin 3-O-b-D-glucopyranoside, regioisomer cleomiscosin D, a inconsequential coumarino-lignan, glucocleomin and glucocapparin, lupeol, camphene, α , β -pinene, p-cymene, myrcene, Cleomiscosin A, B, C, D, E-ocimene, limonene, allo-ocimene, α -terpeniol, α -amorphene, cedrene, citronellic acid, Nevirapine, ethyl palmitate, dehydrolinaloolinoleic acid and palmitic, linolinic oleic, stearic acids (Songsak and Lockwood 2002; Ahmed et al. 2011; Chatterjee et al. 2013; Upadhyay 2015, Mali 2010; Phan et al. 2016).

Imperatorin ([9-(3-methylbut-2-enyloxy)-7H-furo [3, 2-g] chromen-7-one]) is a major active ingredient of Apiaceae and Rutaceae families. Based on the literature survey, imperatorin has been also isolated from *Foeniculum vulgare* *Angelica dahurica* roots (Gyawali and Kang 2018) *Angelica sinensis* and fruits of *Anemone sylvestris*, *Peucedanum praeruptorum*, *Angelica arcangelica* (Cao et al. 2013; Lin et al. 2016), *Casimiroa edulis* leaf (Awaad et al. 2012), *Cnidium monnieri*, *Aralia cordata*, *Angelica dahurica* (Zhao et al. 2022), *Althea officinalis*, *Citrus* fruits (*Citrus limonum*), *Radix glehniae* and *Heracleum rapula* (Lu et al. 2012). It has been reported to possess a wide range of biological activities such as anti-inflammatory, anticancer, analgesic, anticoagulant, antidiabetic, hepatoprotective, and immunomodulatory activities (Kozioł and Skalicka-Woźniak 2016, Mali 2010).

The present study deals with the first report of the compound imperatorin isolated from *C. viscosa*. The crystal compound (imperatorin) was isolated from the aerial parts of *C. viscosa*, characterized through single-crystal XRD, FTIR, and ESI-MS, and further evaluated for antibacterial properties against both Gram +ve and Gram -ve organisms.

2. Results and discussion

Dried powdered aerial parts of *C. viscosa* were subjected to silica gel column chromatography by using gradually increasing polarity solvents through the proportion of H:C, C:EA, EA:M and M. In total 120 fractions were collected, and each fraction was evaporated to aridness beneath room temperature and pooled with similar fractions. Fraction VI showed an obvious spot with an R_f value of 0.584 (imperatorin) in the analysis of TLC which indicates the presence of a pure compound. The imperatorin isolated was carefully crystallized from fraction VI through a mixture of solvents at a ratio of H:EA:M (1.5:0.3:0.2). The UV absorption spectrum showed various absorption peaks with characteristic maxima of imperatorin at 230 nm. The solubility of the isolated and purified bioactive compound was verified and tested using ethanol, chloroform, toluene, methanol, DMSO, and hot water, and it was completely dissolved. Fig. S1 depicts the single pure crystal-XRD of isolated bioactive compound imperatorin. Based on the previous literature, methanolic extracts of *Citrus trifoliata* seeds and fruits were analyzed by using silica gel column chromatography (Kerekes et al. 2022). Likewise, Bertin et al. (2014) reported the isolation of yellow amorphous powder from methanolic extracts of *Casimiroa* genus (Bertin et al. 2014). On the other hand, intensification of imperatorin extraction from *Aegle marmelos* by ultrasound assisted three phase partitioning was reported by Sonar et al. two years ago (Sonar et al. 2021). The crystallized compound in triclinic Pi space collection through four molecules in the component cell ($a = 11.0659(7)$ Å, $b = 11.8277(8)$ Å, $c = 11.9252(9)$ Å,

$\alpha=64.924(4)^\circ$, $\beta=83.661(4)^\circ$, $\gamma=89.247(4)^\circ$ and $Z=4$) was elucidated by X-ray crystallography. From this chromatographic step, not all the secondary metabolites could be identified since several mixtures of different compounds were present (Deposition number CCDC NO: 1883930).

The bond lengths and torsion angles of compound principles are presented in [Tables S1-S3](#). As can be appreciated in [Fig. S1](#), the asymmetric component consists of two autonomous molecules ($Z'=2$). In the two independent molecules, there is no change in the main moiety unlike the side chain moiety. The furochromene ring systems are in planar conformation. The methyl butan side chain moiety is attached to the phenyl ring of chromene moiety. The methyl butan moiety is an extended conformation with the chromene ring system in molecule II, torsion angle $C21-O8-C28-C29=176.2(2)^\circ$. In molecule I, the C13 atomic position was changed from molecule II as can be appreciated from the torsion angle of $C6-O4-C12-C13=62.3(1)^\circ$. In the crystal packing, the structure of molecular is stabilized through $C-H\cdots O$, $C-H\cdots \pi$ and $\pi\cdots\pi$ interactions ([Table S4](#)). The molecules I and II appearance the supramolecular perpetuity layer beside the [100] plane in the complete structure of crystal as shown in [Fig. S2](#). The $C3-H3\cdots O6$ and $C3-H3\cdots O7$ intermolecular electrostatic hydrogen bond interactions are supramolecular layer forms along with [0 1 0] plane as shown in [Fig. S3](#). In these two interactions, atom C3 acts as the bifurcated donor atom and generates an R12(4) graph-set circle pattern in the arrangement. The $C2-H2\cdots O8$ and $C18-H18\cdots O4$ interaction connect A—B—A—B—A—B through C (6) chain running along the "b" axis. The $C2-H2\cdots O8$ and $C3-H3\cdots O6$ electrostatic H bond connections create an R22(8) graph-set circle pattern in the arrangement along with [0 1 0] plane The molecules flanking are simultaneous through $C11-H11\cdots O1$ in molecule I and $C17-H17\cdots O7$ in molecule II intermolecular H bonds forms C (9) perpetuity chains successively beside "a" axis is showed. The $C3-H3\cdots O7$ and $C17-H17\cdots O7$ intermolecular hydrogen bonds comprise a couple of bifurcated acceptor bonds and the $C2-H2\cdots O8$ and $C11-H11\cdots O1$ interactions generating an R44(19) graph-set circle motif equivalent to [0 1 0] plane. The electronegative atom O1 acting as the bifurcated acceptor hydrogen bonds ($C11-H11\cdots O1$ & $C25-H25\cdots O1$) and the $C18-H18\cdots O4$ intermolecular interaction generating an R33(14) ring design in the arrangement. The $C17-H17\cdots O7$, $C18-H18\cdots O4$ and $C26-H26\cdots O4$ intermolecular interactions together form an R33(9) graph-set circle motif in the arrangement. The molecules are linked by pairs of $C25-H25\cdots O1$ and $C26-H26\cdots O4$ intermolecular H bonds, forms an R22(10) ring motif. The 2 molecules are as well supposed jointly through $C-H\cdots \pi$ connections which supply to the aggregation of supramolecular. The $C15-H15\cdots Cg9$ communication with the division remoteness between the acceptor and donor being $3.715(6)$ Å. The molecules in the crystal stacked in layers supposed collectively by $\pi\cdots\pi$ interaction, with the detachment of $Cg2\cdots Cg3$, $Cg7\cdots Cg8$, and $Cg7\cdots Cg9$ are $3.6921(19)$ Å, $3.6061(19)$ Å and $3.613(2)$ Å, respectively as shown in [Fig. S4](#) viewed down "c" axis.

Hirshfeld surface analysis

From the Crystallographic Information File (CIF), a complete structural description helps to quantify and visualize the creature category of intermolecular connections and their collision on crystal stuffing in the surroundings of crystal with the help of

Hirshfeld Surface Analysis by using Crystal Explorer (17.5 software). The plot d_{norm} indicates the remoteness from exterior nuclei surface (d_e) and within the exterior (d_i); on the three-dimensional (3D) Hirshfeld surfaces, the white exterior describes the sum of the vdw radii, blue exterior represents short connect distances compared to the vdw radii, and the red surface represents close contact interactions (H bond contacts). The numerous types of intermolecular connections of molecule in crystal can be identified through the fingerprint plots shapes. The fingerprint plots (2D) facilitate in characterizing contact distances to HSA, which have revealed the range from 0.6 to 2.8 Å including reciprocal contacts. The fingerprint plot and percentage graph shown in the picture serve to measure the influence of various solid-state interactions. If the fingerprint map is compared to molecules 1 and 2, they are almost identical. Because the H--H, O--H, and C--H types of interactions are prominent in both molecules, it is further evidence that the Vander Walls and C--H-- π interactions are crucial to the crystal environment. Both molecules' H--H and O--H contributions are 50.4/44.8 and 27.5/30.5%, respectively. The H--H plot extends beyond occupied fingerprint plots that would typically split from one another, the O--H plot resembles sharp spikes, and the C--H fingerprint plots exhibit comparable symmetrical wing shapes. Compound 1 has significantly lower C--H and O--H contributions than compound 2, and slightly larger H--H contributions. This fingerprint plot thus verifies that the compound's stability in the crystal phase is caused by the presence of weaker hydrogen bonds.

Density functional analysis

DFT is used to determine some basic quantum chemical parameters as well as their geometrical shape. And, E_{HOMO} and E_{LUMO} are essential parameters used to recognize the electronic structure of the ligand to comprehend the geometry conformational of the molecule. Through using Gaussian09 software, the Mullikan infinitesimal charges (MPA) for the imperatorin molecule in the gas phase and vigorous site was considered. The MPA charge of H atoms exhibits high negative charges and carbon atoms carry high positive charges because of which are covalently bonded with an electronegative atom of oxygen. Each atom's charges were varied in the active site lifted molecules compared with gas-phase molecules due to the effect of the protein environment. The moment of dipole together forms the imperatorin molecule has been considered from different quantum chemical methods. The molecule's dipole moment in the gas phase was 6.74D, despite the comparable value in the active site was 4.28/6.21 D. As a result, the lifted molecule's dipole moment in the active site is relatively reduced when compared to that of the imperatorin molecule in the gas phase. This suggests facilitating that after a molecule is nearby in the surroundings of a vigorous site, its dipole moment drops. The direction of the dipole instant vectors in the gas phase and the vigorous site of SAH is shown in the overlaid form of the imperatorin molecule in the gas phase and the dynamic site (Figs. S5-S7). Excitingly, the combination of nucleophilic (concerned with areas with positive budding) and electrophilic (involved just before regions with negative potential) parts of the molecule aids in the electrostatic probable (ESP) map's ability to forecast the probable automatic sites of complexes. The imperatorin molecule's

vital quantum element descriptors, such as the uppermost engaged molecular detour (HOMO) and smallest untenanted molecular detour (LUMO), which are closely associated with biological and chemical activities, were computed. Fig. S8 depicts the molecular surfaces of the two complexes at 0.2 au. The LUMO and HOMO live-ness surfaces were located ended the keto collection and midpoint band regions, correspondingly. The positive and negative areas are represented by the colors red and green, respectively. To comprehend the quantum chemical characteristics, the global reactivity descriptors were derived. It is discovered that the estimated values for LUMO and HOMO energies are, respectively, -6.09 eV and -1.98 eV. There is a -4.11 eV bandgap. The molecule's predicted electronegativity, ionization potential, and electron affinity are 1.98, 6.09, and 4.03 eV, respectively. When compared to the ionization potential, the affinity of electrons and electronegativity principles are stumpy, which signals strong reactivity.

Imperatorin characterization

The FT-IR range of the spectrum shows the characteristic a strapping and pointed quivering band peaks at 3417, 3373, 3289, 2723, 1670, 1614, 1514, 1359, 1316, 1243, 1212, 1165, 1141, 1095, 1011, 1001, 933, 881, 846, 820, 806, 789, 706, 690, 635, 597, 519, 496, 436, 425 and 408cm^{-1} which strength be owing to the presence of -NH, =C-H, -OH, C=C, -CH,-C=O, -CH (bending), -C-O (broaden) -CN (stretch), groups. The different peaks and functional groups and their assignment of isolated compound (imperatorin) are shown in Fig. S9. Besides, the MS spectrum scan was acquired run in positive ionization mode (Fig. S10). Based on the spectral data and in accordance with previous literature data the isolated compound can be inferred as imperatorin (molecular formula: $\text{C}_{16}\text{H}_{14}\text{O}_4$). Similar results were obtained IR spectra showed absorption bands at 3410 (-OH), 1655 (a,b-unsaturated carbonyl group), 1613 (aromatic C,C), 3290cm^{-1} attributed to hydroxyl (OH) functionalities.

Antibacterial activity

The antibacterial activities were tested for different concentrations of isolated imperatorin and were determined by the conventional well diffusion method considering both by Gram-positive and Gram-negative against human pathogenic bacteria. The increasing concentrations of imperatorin (10-40 $\mu\text{g}/\text{mL}$), showed increased inhibitions, as highlighted in Table S5. Imperatorin showed highest activity at 40 $\mu\text{g}/\text{mL}$ concentration against Gram+ve bacteria: *S. aureus* (3 ± 0.2 mm), *B. subtilis* (3 ± 0.6 mm), and Gram -ve bacteria: *K. pneumoniae* (3 ± 0.2 mm), *E. coli* (5 ± 0.2 mm). The screening and isolation of secondary metabolites against different diseases can unlock an original entryway to tackle therapeutically demanding ailments. Based on the above results, *Angelica lucida*, *Magydaris tomentosa* have strong antimicrobial activity with both Gram-bacteria and Gram-negative bacteria (Widelski et al. 2009)

Experimental set-up

Supplied in [supplementary materials](#).

Conclusions

The current work mainly focused on the isolation of bioactive compounds from *C. viscosa*. The proposed method is cheap, non-toxic, reproducible, and eco-friendly. Imperatorin showed a remarkable inhibitory activity against Gram +ve and Gram -ve human pathogens. The chemical characterization might further pave the way for understanding its potential bioactivity and other application like anticancer, antioxidant, anti-inflammatory activities. Our study concludes that the crystal compound is highly effective with antibacterial properties that would be very useful for potential medical applications.

Acknowledgments

We thank the Director, CAS in Botany, University of Madras, Guindy Campus, Chennai for providing facilities to complete the work. For financial assistance we thank the UGC-UPE (Phase II). The instrumentation facility, SAIF, IIT Madras is thanked for support with the spectral analysis.

Disclosure statement

No potential conflict of interest was reported by the authors.

Funding

The author(s) reported there is no funding associated with the work featured in this article.

References

- Ahmed S, Sultana M, Hasan MM, Azhar I. 2011. Analgesic and antiemetic activity of *Cleome viscosa*. Pak J Bot. 43:119–122.
- Awaad AS, Al-Jaber NA, Soliman GA, Al-Outhman MR, Zain ME, Moses JE, El-Meligy RM. 2012. New biological activities of casimiroa edulis leaf extract and isolated compounds. Phytother Res. 26:452–457.
- Bądziul D, Jakubowicz-Gil J, Paduch R, Główniak K, Gawron A. 2014. Combined treatment with quercetin and imperatorin as a potent strategy for killing HeLa and Hep-2 cells. Mol Cell Biochem. 392(1–2):213–227.
- Bertin R, Chen Z, Martínez-Vázquez M, García-Argaéz A, Frolidi G. 2014. Vasodilation and radical-scavenging activity of imperatorin and selected coumarinic and flavonoid compounds from genus Casimiroa. Phytomedicine. 21(5):586–594.
- Cao Y-J, He X, Wang N, He L-C. 2013. Effects of imperatorin, the active component from radix angelicae (Baizhi), on the blood pressure and oxidative stress in 2K,1C hypertensive rats. Phytomedicine. 20(12):1048–1054.
- Chatterjee A, Chattopadhyay SK, Tandon S, Kaur R, Gupta AK, Maulik PR, Kant R. 2013. Isolation of a unique dipyrro-dodiazepinone metabolite nevirapine during large scale extraction of Cliv-92 from the seeds of *Cleome viscosa*. Ind Crop Prod. 45:395–400.
- Ekor M. 2014. The growing use of herbal medicines: issues relating to adverse reactions and challenges in monitoring safety. Front Pharmacol. 4:177.
- Gyawali A, Kang Y. 2018. Blood-to-retina transport of imperatorin involves the carrier mediated transporter system at the inner blood-retinal barrier. J Pharm Sci. 108(4):1–8.

- Kerekes D, Horváth A, Kúsz N, Lajos Borcsa B, Szemerédi N, Spengler G, Csupor D. 2022. Coumarins, furocoumarins and limonoids of *Citrus trifoliata* and their effects on human colon adenocarcinoma cell lines. *Heliyon*. 8(9):e10453.
- Kozioł E, Skalicka-Woźniak K. 2016. Imperatorin—pharmacological meaning and analytical clues: profound investigation. *Phytochem Rev*. 15(4):627–649.
- Lin C-L, Hsiao G, Wang C-C, Lee Y-L. 2016. Imperatorin exerts antiallergic effects in Th2-mediated allergic asthma via induction of IL-10-producing regulatory T cells by modulating the function of dendritic cells. *Pharmacol. Res*. 110:111–121.
- Lu W, Lu Q, Shen S, Wang H, Zhou L, Yu S, Wang H, Jiang H, He L, Zeng S. 2012. Simultaneous determination of imperatorin and its 2 metabolites in dog plasma by using liquid chromatography–tandem mass spectrometry. *J Pharm Biomed Anal*. 70:640–646.
- Mali RG. 2010. *Cleome viscosa* (wild mustard): a review on ethnobotany, phytochemistry, and pharmacology. *Pharm. Biol*. 48(1):105–112.
- Phan NM, Nguyen TP, Dung Le T, Chi Mai T, Thanh Phong M, Tri Mai D. 2016. Two new flavonol glycosides from the leaves of *Cleome viscosa* L. *Phytochem Lett*. 18:10–13.
- Singh H, Ali SS, Khan NA, Mishra A, Mishra AK. 2017. Wound healing potential of *Cleome viscosa* L seeds extract and isolation of active constituent. *South Afr J Bot*. 112:460–465.
- Sonar MP, Kumar D, Nikam D, Rathod VK. 2021. Intensification of imperatorin extraction from *Aegle marmelos* by ultrasound assisted three phase partitioning: comparative studies and exploring its ethnomedicinal uses. *Chem Eng Process Process Intensification*. 169:108588.
- Songsak T, Lockwood GB. 2002. Glucosinolates of seven medicinal plants from Thailand. *Fitoterapia* 73:209–216.
- Upadhyay RK. 2015. *Cleome viscosa* Linn: a natural source of pharmaceuticals and pesticides. *Int J Green Pharm*. 9(2):71–85.
- Widelski J, Popova M, Graikou K, Glowinski K, Chinou I. 2009. Coumarins from *Angelica Lucida* L. - antibacterial activities. *Molecules*. 14(8):2729–2734.
- Yadav NP, Chanda D, Chattopadhyay SK, Gupta AK, Pal A. 2010. Hepatoprotective effects and safety evaluation of coumarinolignoids isolated from *Cleome viscosa* seeds. *Indian J Pharm Sci*. 72(6):759–765.
- Zhao H, Feng Y-L, Wang M, Wang J-J, Liu T, Yu J. 2022. The *Angelica dahurica*: A review of traditional uses, phytochemistry and pharmacology. *Front Pharmacol*. 13:896637.